J Mater Sci: Mater Med (2008) 19:2535–2540
DOI 10.1007/s10856-007-3089-3

Selective laser sintering of porous tissue engineering scaffolds from poly(L-lactide)/carbonated hydroxyapatite nanocomposite microspheres

Wen You Zhou · Siu Hang Lee · Min Wang · Wai Lam Cheung · Wing Yuk Ip

Received: 6 March 2007 / Accepted: 10 May 2007 / Published online: 10 July 2007

Abstract This study focuses on the use of bio-nanocomposite microspheres, consisting of carbonated hydroxyapatite (CHAp) nanospheres within a poly(L-lactide) (PLLA) matrix, to produce tissue engineering (TE) scaffolds using a modified selective laser sintering (SLS) machine. PLLA microspheres and PLLA/CHAp nanocomposite microspheres were prepared by emulsion techniques. The resultant microspheres had a size range of 5–30 μm, suitable for the SLS process. Microstructural analyses revealed that the CHAp nanospheres were embedded throughout the PLLA microsphere, forming a nanocomposite structure. A custom-made miniature sintering platform was installed in a commercial Sinterstation® 2000 SLS machine. This platform allowed the use of small quantities of biomaterials for TE scaffold production. The effects of laser power; scan spacing and part bed temperature were investigated and optimized. Finally, porous scaffolds were successfully fabricated from the PLLA microspheres and PLLA/CHAp nanocomposite microspheres. In particular, the PLLA/CHAp nanocomposite microspheres appeared to be promising for porous bone TE scaffold production using the SLS technique.

Introduction

Bone replacements are frequently required for damaged bone tissue due to trauma, cancer, and more generally in surgeries [1, 2]. This requirement for bone tissue repair is a major clinical and socioeconomic need. At present, many injuries are not adequately treated because bone defects above a critical size cannot be repaired through natural healing [3]. Bone repair is limited by supply constraints and morbidity associated with autograft and allograft. The advent of tissue engineering (TE) in the late 1980s represents a promising approach to overcoming the various limitations of current bone grafting methods [4]. Tissue engineering, in general, needs the implantation of a biocompatible and biodegradable porous scaffold, which serves as a temporary template for cell attachment, development and subsequent tissue generation. The scaffold plays a crucial role in bone tissue engineering and its architecture defines the final shape of the new bone. Thus, the success of bone TE depends, to a large extent, on the performance of the 3D biodegradable scaffold.

Bone TE scaffolds can be fabricated from both synthetic and naturally derived biodegradable polymers such as poly(L-lactide) (PLLA) [5], poly(ε-caprolactone) (PCL) [6] and chitosan [7]. Bone itself is an inorganic–organic nanocomposite. Recently, more and more researches emphasize on the use of engineered composite bone scaffolds, which combine the strength and stiffness of bioactive inorganic fillers with the flexibility and toughness of biodegradable organic matrices [8–10]. The selection of appropriate biomaterials for producing the scaffolds is a very important step because the scaffold properties are largely determined by the intrinsic properties of the materials. However, the scaffold design and processing method will also play an important role in porosity, mechanical properties and degradation behavior.

Recent advances in rapid prototyping (RP) technologies have allowed tissue engineers to design and fabricate scaffolds with a highly complex and completely interconnected pore network. A natural extension of RP is rapid

W. Y. Zhou · S. H. Lee · M. Wang · W. L. Cheung (✉)
Department of Mechanical Engineering, The University of Hong Kong, Pokfulam Road, Hong Kong, China
e-mail: wlcheung@hku.hk

W. Y. Ip
Department of Orthopaedics and Traumatology, The University of Hong Kong, Sassoon Road, Hong Kong, China

manufacturing (RM), the automated manufacture of end-use products or near finished parts directly from CAD data. The potential advantages of RM in production of TE scaffolds include the following: (1) fewer design constraints, (2) customization (patient-specific), (3) faster manufacture speed, (4) functionally graded materials, (5) free of toxic solvents and (6) controllable and reproducible structures and porosity [11].

Among various RP technologies, selective laser sintering (SLS) has been found to be advantageous for TE scaffold fabrication due to its ability to process a wide range of biocompatible and biodegradable materials [12]. In the SLS process, 3D computer images are sectioned into thin 2D layers (~0.1 mm thick) and the 3D objects are built layer-by-layer to the required size, shape and internal structure by laser-induced fusion of small particles of ceramic, metal or thermoplastic powders. So far, only PCL biodegradable polymer has been used to produce TE scaffolds by SLS because it is significantly less expensive than other biodegradable polymers and supplied in fine powder form [13–15]. Recently Wiria et al. [16] applied the SLS technique to first fabricate biodegradable composite scaffolds from physically blended PCL with micro-sized hydroxyapatite.

Although SLS is a promising technology for TE scaffold fabrication, so far it is not economical to use commercial SLS machines to process most biopolymers because the amount of material required is quite large and they are still very expensive and not in the appropriate powder form. The objective of this study was to modify an existing Sinterstation® 2000 SLS system in order to produce TE scaffolds using small quantities of biomaterial powders. Porous bone TE scaffolds were sintered from in-house made PLLA microspheres and PLLA/carbonated hydroxyapatite (CHAp) nanocomposite microspheres using the modified SLS machine. Very promising results have been obtained.

Materials and processing

Preparation of PLLA microspheres

The PLLA used was Medisorb® 100L 1A (Lakeshore Biomaterials, AL, USA) with an inherent viscosity of 1.9 dL/g. A DSC analysis showed that it has a glass transition temperature (T_g) of 66.7 °C and a melting temperature (T_m) of 176.5 °C. It was supplied in the form of macro-sized pellets, 1 mm in diameter and 3 mm in length, which was suitable for conventional extrusion and molding processes but not for selective laser sintering. PLLA microspheres were prepared using a normal oil-in-water (O/W) emulsion/solvent evaporation technique. Poly(vinyl alcohol) (PVA, Sigma-Aldrich, cold water soluble) was used as the emulsifier and dichloromethane (A.R. grade) used as the organic solvent to dissolve PLLA. The resultant PLLA microspheres were washed and lyophilized to get dry powder.

Preparation of PLLA/CHAp nanocomposite microspheres

The carbonated hydroxyapatite nanospheres were synthesized in-house by a nanoemulsion method [17]. The mean particle size of the CHAp particles was about 20 nm. The PLLA/CHAp nanocomposite microspheres were prepared using a solid-in-oil-in-water (S/O/W) emulsion/solvent evaporation method as reported earlier [18]. Briefly, the CHAp nanospheres were dispersed in the PLLA-dichloromethane solution by ultrasonification and homogenization to form an S/O nanosuspension. The nanosuspension was mixed with PVA solution to prepare the PLLA/CHAp nanocomposite microspheres. In this study, only nanocomposite microspheres containing 10 wt% CHAp were used in the scaffold production.

Modification of Sinterstation® 2000 system

In order to reduce the consumption of biomaterial powders for TE scaffold construction in the SLS process, modifications were made to an existing Sinterstation® 2000 SLS machine (3D Systems, Valencia, CA, USA). The CO_2 laser of the system has a maximum power output of 50 watts. The CO_2 laser energy intensity across the beam diameter very nearly follows the Gaussian distribution [19]. A miniature sintering platform, which consisted primarily of a miniature build cylinder and two powder supply chambers, was designed, fabricated and installed in the build cylinder of the existing SLS machine [20]. The miniature build cylinder had a diameter of 49 mm and the movement of its base was directly linked to the base of the existing build cylinder of the Sinterstation® 2000 system. The two powder supply chambers were driven by two additional stepping motors beneath the miniature sintering platform. In the sintering processes, the original powder supply tanks of the Sinterstation® 2000 system were empty and small amounts of biomaterial powder were fed from the miniature powder supply chambers. The roller positions were sensed and the signals were fed to a control panel which controlled the movement of stepping motors and the temperature of the small build cylinder. Other sintering parameters were controlled by the existing Sinterstation® 2000 system and this would ensure good quality of the scaffolds built.

Scaffold design and fabrication

A tetragonal porous scaffold model ($L \times W \times H = 8 \times 8 \times 16$ mm^3) was designed by an extrude-cut patterning method using SolidWorks® (version 2005). Rectangular channels of the same size were cut in all three dimensions to form 3D symmetrical scaffold models. This simple design contains the typical features and features sizes found in bone TE scaffolds [15]. In SLS of porous scaffolds, the spot size of the laser beam is very important for building the small features of the scaffolds. The spot size or beam width is defined as the smallest diameter of the focused laser beam. According to the manufacturer, the spot size of the Sinterstation® 2000 system is 0.018″ (~457 μm). To facilitate handling of the sintered scaffolds, a solid base ($9 \times 9 \times 3$ mm^3) was incorporated in the scaffold design. If this base was not provided, the first few porous layers would tend to warp significantly, affecting the overall quality of the scaffolds. The solid base may also be used as the surgical fixation base structure. The scaffold data file was exported in an STL format and then transferred to the Sinterstation® 2000 system for the sintering process. The build orientation (angle between the laser scanning direction and "L" dimension of the scaffold) was 45°. Significant variation in density and anisotropic properties were found in DuraForm™ polyamide (a common SLS material) parts built in 0° and 90° orientations [21]. The 45° build orientation was chosen to reduce the anisotropy, also it was found to be effective in reducing warpage of the porous scaffolds [22].

In SLS, the laser energy density (ED) level significantly affects the scaffold properties. The ED level is a measure of the amount of energy supplied to the powder particles per unit area of the powder bed surface. The relationship between ED and laser power (P), scan spacing (SS) and beam speed (BS) can be expressed by the following equation [19]:

$$ED = \frac{P}{SS \times BS} \quad (1)$$

It is obvious that too low a laser power will render low strength or even incomplete sintering of the scaffold, while too high a laser power will cause the biopolymer to degrade and the scaffold to warp due to high residual stresses. SS means the distance between two parallel laser scans during a fill. In this study, the BS was fixed at 1257 mm/s and the effects of laser power, scan spacing and part bed temperature (PBT) were investigated. Prior to this study, DuraForm™ polyamide was used as the reference material for initial settings of the sintering parameters. After some trials, a workable set of sintering parameters was obtained for PLLA and PLLA/CHAp nanocomposite as shown in Table 1.

Table 1 Sintering conditions suitable for PLLA and PLLA/CHAp microspheres

Sintering condition	PLLA	PLLA/CHAp
Scan spacing (mm)	0.15–0.21	0.15–0.21
Part bed temperature (°C)	30–40	30–60
Layer thickness (mm)	0.10	0.10
Roller speed (mm/s)	127	127
Scan speed (mm/s)	1257	1257
Stepping motor delay (ms)	120	160
Fill laser power (W)	11–15	11–19

Morphology characterization

The morphologies of the PLLA microspheres and PLLA/CHAp nanocomposite microspheres were examined using a scanning electron microscope (SEM, Cambridge S440). Focused ion beam (FIB, FEI Quanta 200 3D) was applied to section some nanocomposite microspheres for internal examination. The FIB milling process was carried out with a Ga^+ ion beam current of 3nA and the acceleration voltage was 5 KeV. The milled faces were then polished with a low beam current of 0.3 and 0.1 nA prior to SEM imaging. Some sintered scaffolds were also examined by SEM and the samples were sputter coated with Au prior to examination.

Results and discussion

Some PLLA microspheres and PLLA/CHAp nanocomposite microspheres are shown in Fig. 1a and b, respectively. Both types of microsphere exhibited a generally similar range of particle sizes between 5 and 30 μm and which were suitable for SLS process. The pure PLLA microspheres appeared very smooth while some CHAp nanospheres were found partially embedded on the PLLA/CHAp nanocomposite microspheres and this may impart bioactivity (osteoconductivity) for the scaffolds built. Figure 2 shows the FIB-milled section of a PLLA/CHAp composite microsphere. The CHAp nanospheres were generally well distributed both on and inside the microsphere, forming a nanocomposite structure. The rough surfaces of the nanocomposite microspheres will likely facilitate cell attachment. Preliminary nanoindentation tests showed an increase in hardness, probably due to the embedded CHAp nanoparticles. In addition, the nanocomposite microspheres flowed more easily than the pure PLLA microspheres, making powder deposition easier.

Figure 3 shows the effect of PBT on the structure of scaffolds built from the pure PLLA microspheres. When PBT was within the range as shown in Table 1, the unsintered powder within the pores could be removed easily

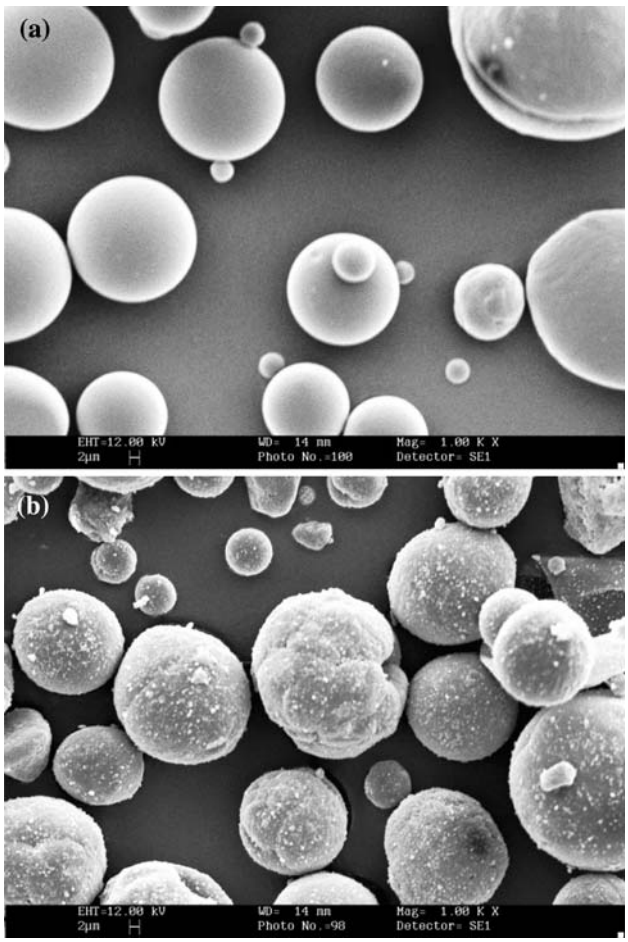

Fig. 1 SEM images of microspheres: (**a**) PLLA and (**b**) PLLA/CHAp nanocomposite

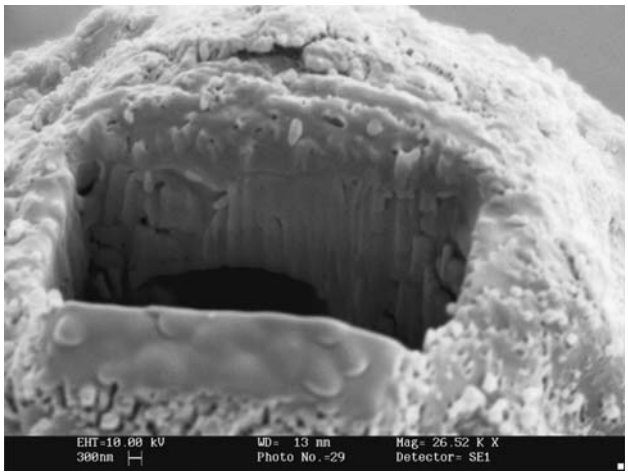

Fig. 2 SEM image of an FIB-milled section of a PLLA/CHAp nanocomposite microsphere

by an air gun and the resultant scaffolds exhibited a distinctive porous structure (sample A). When PBT was higher than the recommended range however it was difficult to remove all the unsintered powder from the pores (sample B). In normal SLS processes, PBT should be set near the T_g of amorphous polymers and just below the T_m of semi-crystalline polymers meanwhile the laser only provides small amounts of extra heat energy for powder fusion. Too high a PBT caused the powder in the pores to partially fuse with the design structure and difficult to be removed. On the other hand, too low a PBT would result in low strength of the scaffolds and they tended to fall apart during handling. Figure 4 shows the effect of SS. Too small an SS would result in excessive amount of laser energy to be dumped on the powder bed surface and cause blocking of the pores (sample A). When SS was too large, the laser energy density became too low for complete sintering of the scaffold structure and hence it could not

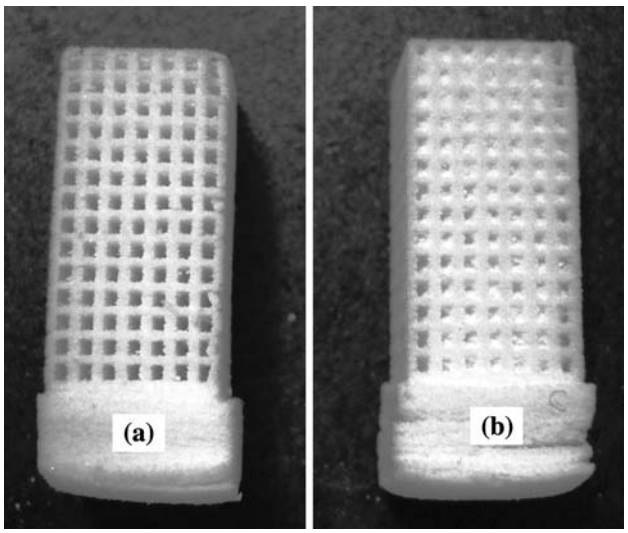

Fig. 3 Effect of part bed temperature (PBT) on structure of PLLA porous scaffolds: (**a**) PBT = 35 °C and (**b**) PBT = 50 °C, other sintering conditions are shown in Table 1

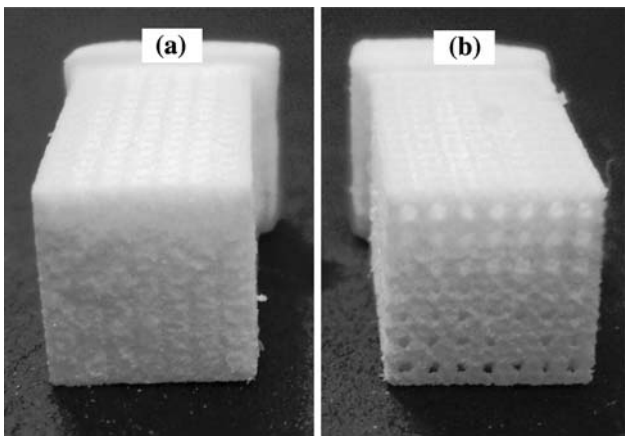

Fig. 4 Effect of scan spacing (SS) on structure of PLLA porous scaffolds: (**a**) SS = 0.08 mm and (**b**) SS = 0.18 mm, other sintering conditions are shown in Table 1

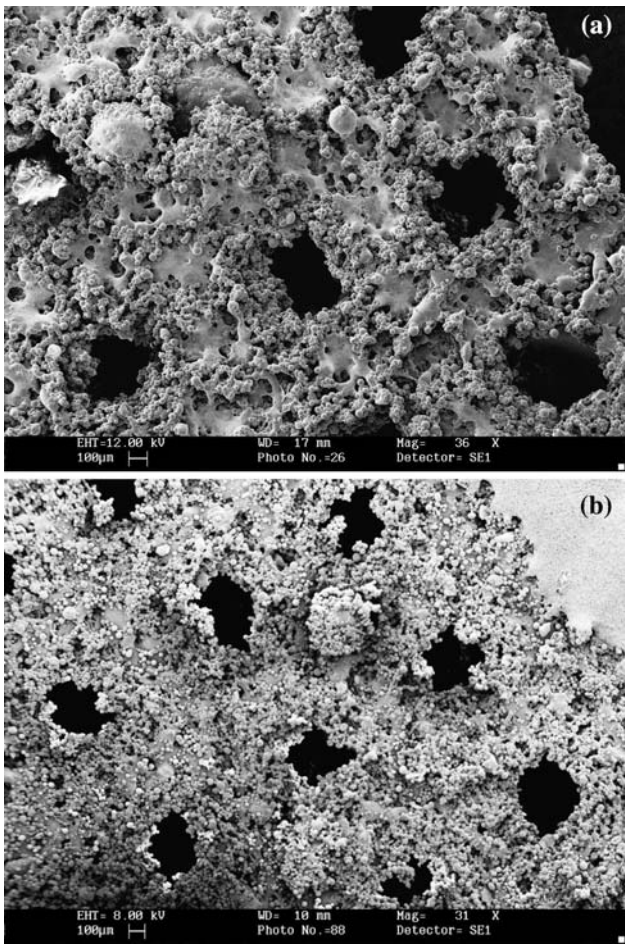

Fig. 5 SEM images showing the layer structures of a PLLA scaffold (**a**) and a PLLA/CHAp nanocomposite scaffold (**b**), sintering conditions are shown in Table 1

take shape. In general, extreme values of the processing parameters should be avoided in order to obtain a desirable porous structure.

Figure 5 shows the typical layer structures of the PLLA and PLLA/CHAp scaffolds sintered under the recommended conditions as listed in Table 1. It can be seen that the PLLA microspheres were well fused in the scanned areas (Fig. 5a). Nevertheless, the sintered material was not fully dense but some very fine pores were present, resulting in a porous structure possessing a combination of macro-pores (design pores) and micro-pores (due to incomplete fusion of the sintered material). This structure likely facilitates the flow of body fluid and promotes nutrition and metabolism waste exchange, and hence is more beneficial to cell growth than a scaffold with only micro-pores, for example the PCL/HAp scaffolds reported by Wiria et al. [16]. Also, the powder preparation methods used in the two studies were different. In this study, the nanocomposite was prepared by emulsion method and the nano-sized CHAp particles were well encapsulated in the PLLA/CHAp microspheres even before sintering, meanwhile the PCL/HAp composites used by Wiria et al. [16] were physically blended. Furthermore, the biopolymers used in the two studies were different; therefore, the scaffolds produced likely have different in vitro and in vivo properties.

It can also be seen from Fig. 5a and b that the degree of fusion of the PLLA/CHAp nanocomposite powder was lower than that of the pure PLLA powder. This could be explained by the increased viscosity of the composite material. Also the CHAp nanoparticles on the powder surface might act as a barrier against fusion. When the scaffolds were sintered with the respective conditions as shown in Table 1, there was no problem in removing the excessive trapped powder from the pores. For the PLLA scaffolds, a low pressure air gun was used to remove the excessive powder. The layers were generally well preserved afterward and the pores of the scaffolds could be clearly identified. For the PLLA/CHAp nanocomposite scaffolds, the loose powder could be shaken off by hand. The general appearance of a PLLA/CHAp porous scaffold after removal of the excessive powder is shown in Fig. 6. Such a solid scaffold can be used for subsequent mechanical and biological assessments. In fact, in vitro study of sintered scaffolds through cell culture is currently being performed. The final point of discussion in this paper is the pore size. There is a difference in the design and actual pore sizes. When the design pore size was 0.8 mm, the actual pore size of sintered scaffolds was only about 0.6 mm. Obviously the reduction in pore size was a result of "growth" which was caused by the penetration of the laser energy beyond the design scan area. Further work is

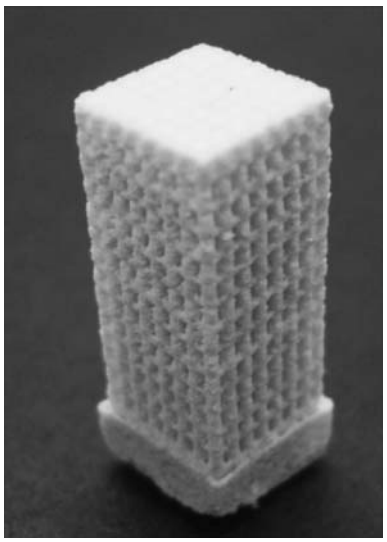

Fig. 6 An isometric view of a PLLA/CHAp nanocomposite scaffold, sintering conditions are shown in Table 1

underway to optimize the processing parameters and to produce good quality scaffolds for various studies.

Conclusions

The PLLA microspheres and PLLA/CHAp nanocomposite microspheres fabricated using the emulsion techniques were found well suited for the SLS process. SEM examination of FIB-milled PLLA/CHAp microspheres revealed that the CHAp nanospheres were generally well dispersed on the surface as well as inside the microspheres to form a nanocomposite structure. The custom-made miniature sintering platform allowed small quantities of the biomaterial powders to be processed in a commercial Sinterstation® 2000 SLS machine. With this platform, prototypes of porous bone TE scaffolds were successfully built from the PLLA and PLLA/CHAp nanocomposite microspheres. The effects of laser power; scan spacing and part bed temperature on the scaffold structure were studied and discussed. In general, extreme values of the processing parameters should be avoided in order to obtain desirable scaffold properties. It has been reported in the literature that removing the excessive powder from the pores is a major obstacle for porous scaffold production using the SLS process. In this study the PLLA/CHAp nanocomposite microspheres seem to offer a solution to the problem provided the sintering conditions are properly set.

Acknowledgement This work was supported by a CERG research grant (HKU 7118/05E) from the Hong Kong Research Grants Council.

References

1. P. SEPULVEDA, J. R. JONES and L. L. HENCH, *J. Biomed. Mater. Res.* **59** (2002) 340
2. M. NAVARRO, S. DEL VALLE, S. MARTINEZ, S. ZEPPETELLI, L. AMBROSIO, J. A. PLANELL and M. P. GINEBRA, *Biomaterials* **25** (2004) 4233
3. M. MARTINA, G. SUBRAMANYAM, J. C. WEAVER, D. W. HUTMACHER, D. E. MORSE and S. VALIYAVEETTIL, *Biomaterials* **26** (2005) 5609
4. C. T. LAURENCIN and H. H. LU, in *"Bone Engineering"* edited by J. E. Davies (Em Squared, Toronto, Canada, 2000) p. 462
5. V. J. CHEN, L. A. SMITH and P. X. MA, *Biomaterials* **27** (2006) 3973
6. H. YOSHIMOTO, Y. M. SHIN, H. TERAI and J. P. VACANTI, *Biomaterials* **24** (2003) 2077
7. A. DI MARTINO, M. SITTINGER and M. V. RISBUD, *Biomaterials* **26** (2005) 5983
8. F. NAGATA, T. MIYAJIMA and Y. YOKOGAWA, *Key Eng. Mater.* **254–256** (2004) 293
9. S. S. KIM, M. SUN PARK, O. JEON, C. YONG CHOI and B. S. KIM, *Biomaterials* **27** (2006) 1399
10. K. REZWAN, Q. Z. CHEN, J. J. BLAKER and A. R. BOCCACCINI, *Biomaterials* **27** (2006) 3413
11. M. M. SAVALANI and R. A. HARRIS, *Proc. Inst. Mech. Eng. H* **220** (2006) 505
12. C. K. CHUA, K. F. LEONG, K. H. TAN, F. E. WIRIA and C. M. CHEAH, *J. Mater. Sci. Mater. Med.* **15** (2004) 1113
13. G. CIARDELLI, V. CHIONO, C. CRISTALLINI, N. BARBANI, A. AHLUWALIA, G. VOZZI, A. PREVITI, G. TANTUSSI and P. GIUSTI, *J. Mater. Sci. Mater. Med.* **15** (2004) 305
14. J. M. WILLIAMS, A. ADEWUNMI, R. M. SCHEK, C. L. FLANAGAN, P. H. KREBSBACH, S. E. FEINBERG, S. J. HOLLISTER and S. DAS, *Biomaterials* **26** (2005) 4817
15. B. PARTEE, S. J. HOLLISTER and S. DAS, *J Manuf Sci E* **128** (2006) 531
16. F. E. WIRIA, K. F. LEONG, C. K. CHUA and Y. LIU, *Acta Biomater.* **3** (2007) 1
17. W. Y. ZHOU, M. WANG, W. L. CHEUNG, B. C. GUO and D. M. JIA, *J. Mater. Sci. Mater. Med.* DOI: 10.1007/s10856-007-3156-9
18. W. Y. ZHOU, M. WANG and W. L. CHEUNG, *Key Eng. Mater.* **334–335** (2007) 1221
19. J. C. NELSON, S. XUE, J. W. BARLOW, J. J. BEAMAN, H. L. MARCUS and D. L. BOURELL, *Ind Eng Chem Res* **32** (1993) 2305
20. W. Y. ZHOU, S. H. LEE, M. WANG and W. L. CHEUNG, *Key Eng. Mater.* **334–335** (2007) 1225
21. B. CAULFIELD, P. E. McHUGH and S. LOHFELD, *J. Mater. Process. Technol.* **182** (2007) 477
22. S. H. LEE, W. Y. ZHOU, K. LI, M. WANG and W. L. CHEUNG, in Proceedings of the Biomedical Engineering Conference (BME2004), Hong Kong (2004) 91